Available online at www.eccomasproceedia.org
Eccomas Proceedia COMPDYN (2023) 3466-3482

ECCOMAS
Proceedia

COMPDYN 2023
9th ECCOMAS Thematic Conference on
Computational Methods in Structural Dynamics and Earthquake Engineering
M. Papadrakakis, M. Fragiadakis (eds.)
Athens, Greece, 12-14 June 2023

MODELLING STRATEGIES OF INFILL MASONRY WALLS FOR SEISMIC ANALYSIS OF BUILDING STRUCTURES

Pedro P. Folhento[1], Rui C. Barros[1], and Manuel T. Braz-César[2]

[1] CONSTRUCT, Faculdade de Engenharia da Universidade do Porto
Porto, Portugal
{up201811645@edu.fe.up.pt, rcb@fe.up.pt}

[2] CONSTRUCT, Instituto Politécnico de Bragança
Bragança, Portugal
brazcesar@ipb.pt

Abstract

Infill walls in frame structures greatly influence the dynamic behaviour of buildings and consequently their performance when under seismic loads. In building construction, unreinforced masonry walls constitute one of the oldest and worldwide used materials. Despite of great simplicity of their application due to their assemblage process, their behaviour under earthquake events is rather complex, and it is usually neglected in the design phase of building structures. Numerous studies have been conducted over the years to model and assess the influence of non-structural infill walls in buildings. Micro-, meso- and macro-models are available in the literature, although the choice of one of these types of models depends on the problem under consideration. For the current investigation, macro-models are more adequate, in particular equivalent strut models. This kind of modelling has been evolving over the years accounting for a large number of phenomena intrinsic to these elements: the failure modes expected by the infill walls; the relative infill-frame lateral stiffness; the consideration of openings in infills and partially infill walls; bounding frame columns' shear failure; vertical loading effect; out-of-plane behaviour of the infill and its interaction with in-plane behaviour; applicability to multiple degrees-of-freedom systems with multiple stories and bays, etc. This study considers two well-known macro-modelling strategies of unreinforced infill masonry walls in reinforced concrete frame structures modified to improve the in-plane and out-of-plane behaviour simulation under seismic actions. Results showed that these modifications allowed for better reproduction of infill walls' behaviour compared with experimental tests.

Keywords: Infill masonry walls, Non-structural elements, Seismic analysis, Model Validation, Building structures.

ISSN:2623-3347
Peer-review under responsibility of the organizing committee of COMPDYN 2023.
doi: 10.7712/120123.10653.20834

1 INTRODUCTION

Infill masonry walls in frame structures are known for their relevant influence on the dynamic behaviour of building structures and consequently the influence on their performance when subjected to seismic loads. In building construction, unreinforced masonry walls constitute one of the oldest and worldwide used materials. Despite of great simplicity in the application of these non-structural elements due to their assemblage process, their behaviour under earthquake events is rather complex, and thus it is usually neglected in the design phase of building structures. The interaction between the surrounding frame structure and the infill panel is not straightforward, it depends on numerous factors such as brick materials, mortar mechanical characteristics, brick geometry, workmanship quality, relative stiffness between the frame and the infill panel, etc. [1], which contribute for uncertainties in the accurate modelling of such non-structural elements.

Numerous studies have been conducted over the years to model and assess the influence of non-structural infill walls in buildings. Micro-, meso- and macro-models are available in the literature, although the choice of one of these types of models depends on the problem under consideration [1, 2].

The current investigation deals with macro-models, particularly equivalent strut models, which are more adequate for building structures with multiple stories and bays. This kind of modelling has been evolving over the years and can now account for a large number of physical phenomena intrinsic to these elements [3 – 12].

Two well-known macro-modelling strategies of unreinforced infill masonry walls in reinforced concrete (RC) frame structures are considered and modified to improve in-plane and out-of-plane behaviour simulation under seismic actions. The procedures are explained by presenting the modelling choices and assumptions used. The accuracy of such models is verified against different experimental results found in the literature [13 – 15], by calibrating the constitutive parameters of the infill wall elements with the subsequent use of a simplex and genetic algorithm [16].

Results indicate that these modifications allowed for better reproduction of the in-plane and out-of-plane behaviour of infill masonry walls when compared with different experimental tests, being appropriate for the use in numerical models of RC building structures, provided that the models' parameters are adequately chosen and calibrated.

2 MODELLING STRATEGIES

Generally, the bare frame withstands the gravity loads, whilst the frame and infill walls jointly carry the horizontal loads, e.g., winds or earthquakes, with a prevalent truss action mechanism in the infills [1]. Under these conditions, the infills tend to react with the bounding structure between the upper corner of the windward column and the lower corner of the leeward column, resulting in a compression-only diagonal. Large deformations cause the frame and the infill panel to interact at these corner regions (the contact lengths) and to separate in the opposite corners due to the differences in deformation of these elements, producing cracks at these interfaces.

Infill masonry wall macro-models generally consider equivalent diagonal strut elements. The standard strut model usually considers two struts in each direction as represented in Figure 1, functioning in a compression-only fashion. However, this modelling approach has been through an evolutionary process, in which different phenomenological features were added, whether by changing the number and arrangement of the struts and/or attributing different material laws to simulate different kinds of behaviour. Such features may include: the in-plane (IP) failure modes of the infill walls [3, 4]; the relative infill-frame lateral stiffness [5]; open-

ings in the infill panel and partially infill walls [6]; brittle failure of columns of the bounding frame [7]; vertical loading influence [8]; out-of-plane (OOP) stiffness, strength and failure, and its interaction with IP behaviour [9 – 11]; applicability to structural systems as buildings with multiple stories and bay [12], etc.

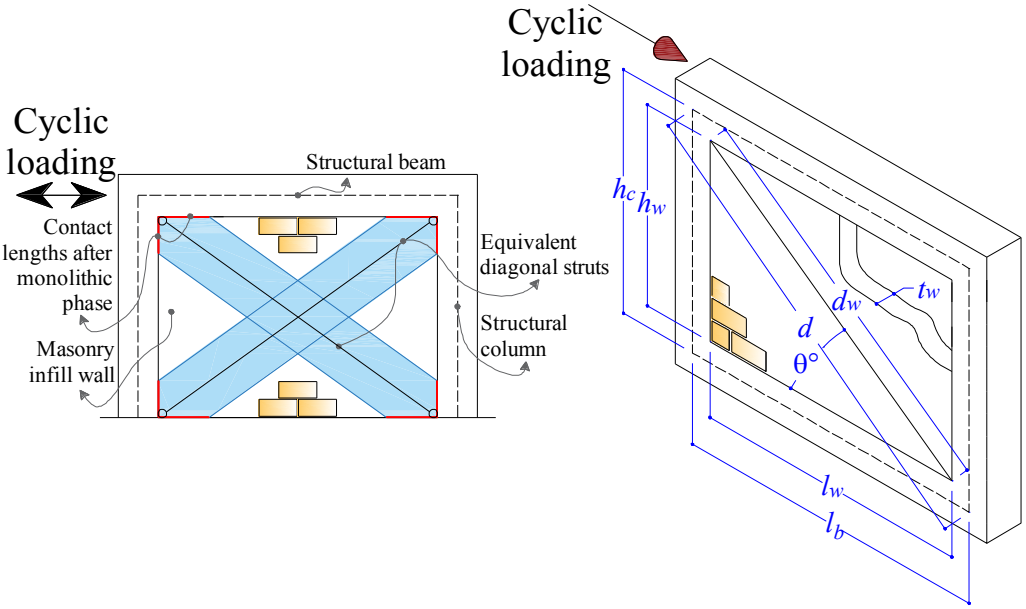

Figure 1: Standard equivalent diagonal strut model.

Among a large number of choices of macro-modelling techniques using equivalent diagonal struts, two approaches were selected for their relevance in the literature: Kadysiewski and Mosalam [9] model and Furtado et al. [10] model represented in Figure 2. Both models account for IP and OOP effects in the infill walls and can consider the collapse of individual infills upon exceedance of certain threshold values of drift. However, and despite the common disadvantage of not considering the possible shear failure of columns in the bounding frame (a disadvantage not addressed at this time), Furtado's model considers OOP linear behaviour and Kadysiewski and Mosalam's model does not properly captures the initial elastic and post-yield softening behaviour of infill walls.

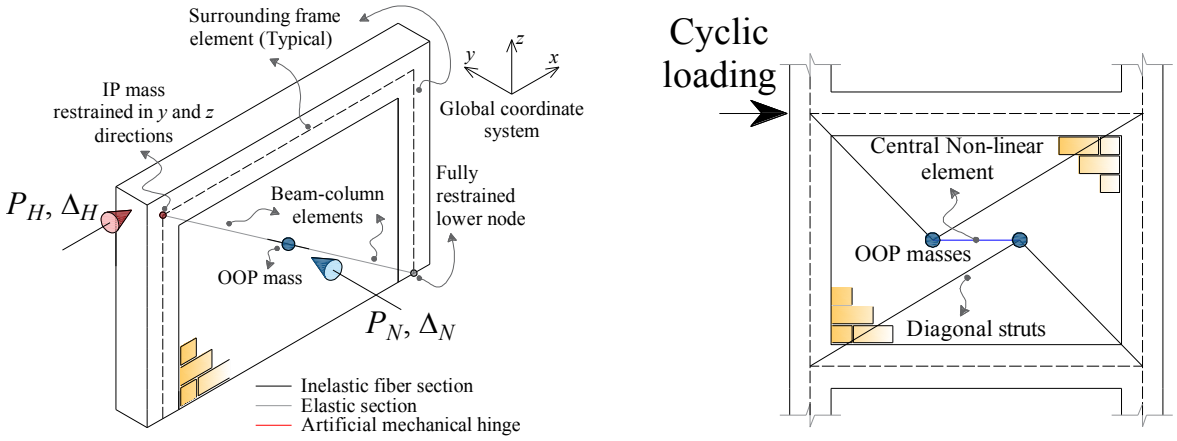

(a) Kadysiewski and Mosalam model; (b) Furtado et al. model.

Figure 2: Adopted modelling strategies for modification.

This study will address these points based on modifications carried out in these modelling techniques [17, 18]. Numerical models are developed using the OpenSees software [19, 20], and the calibration/optimization procedure and postprocessing of results are carried out using MATLAB [21]. Scripts were developed in Python language comprising functions for each of these models. The aim is to develop a model that could represent both the IP and OOP cyclic behaviour of infill masonry walls in RC frame structures using real provided mechanical parameters (when available), and in the absence of these, derivations of such parameters based on empirical assumptions. In addition, a Python function was developed to convert automatically the OpenSeesPy commands written directly to a Tcl file. This Tcl file containing specific information about the model will work as a batch file to be interpreted by MATLAB and used in parallel computing for model optimization and calibration purposes.

To model the RC beams and columns, force-based beam-column finite elements are used [22] with finite-length lumped plasticity using the modified Gauss-Radau plastic hinge integration method [23] and the Paulay and Priestly [4] expression to calculate the plastic hinge length in beams and columns. Linear geometric effects are considered by introducing the P-Δ term in the equilibrium upon geometric transformation [24]. The uniaxial materials are assigned to the different fibres in the critical sections following the Kent-Scott-Park model [25] for confined and unconfined concrete (respectively, *Concrete02* and *Concrete01* uniaxial materials in OpenSees) and a hysteretic law for the steel reinforcement (using the *Hysteretic* uniaxial material in OpenSees) that considers strength hardening and stiffness degradation. A cyclic shear law is also aggregated as a uniaxial material to the critical sections of columns, accounting for shear deformations and the possible shear failure in columns. All models are developed in a three-dimensional environment, so that elastic torsion is also included by aggregation to the element sections.

For both models a backbone curve of IP force-displacement as represented in Figure 3a is defined considering cracking, yielding, maximum, and ultimate points. However, this backbone is applied and used differently for each model as will be explained in the further two subsections.

Cracking and maximum IP forces are, respectively, calculated as follows [3, 4]

$$V_{\max} = \min\left(\underbrace{\frac{2}{3} z\, t_w\, f_m \sec(\theta)}_{R_{DC}\text{ (Diagonal compression)}} , \underbrace{\frac{\tau_0}{1 - \mu\left(h_c / l_b\right)} t_w\, d_w}_{R_{SS}\text{ (Shear sliding)}} \right) \cos(\theta) \tag{1}$$

$$V_{\text{crack}} = 0.5\pi t_w\, d_w\, f_{tm} \cos(\theta) \tag{2}$$

in which μ is the coefficient of friction [26], z is the columns to infill contact lengths, and λ [5] is the frame-infill relative stiffness parameter, respectively,

$$z = \frac{\pi}{2} \frac{h_c}{\lambda} \quad \text{and} \quad \lambda = \sqrt[4]{\frac{E_{m0} t_w \sin(2\theta)}{4 E_c I_c h_w}} \tag{3}$$

where f_{tm} is the masonry tensile strength, assumed as 5% of masonry compressive strength along the mortar bed-joints [27], f_{m0}, and f_{m0} depending on the direction of voids in the masonry units is herein assumed to suffer an increase or reduction of 20% compared with the compressive strength of masonry perpendicular to the mortar bed-joints, f_{m90}. The Young's modulus of the masonry material along, E_{m0}, and orthogonal to the bed joints, E_{m90}, were computed in function of masonry compressive strength and the shear modulus, $G_{m0\text{-}90}$ (=0.4E_{m90}), implicitly assuming the Poisson's ratio, $\nu_{m0\text{-}90}$, as 0.25 [28]. A homogenous ortho-

tropic behaviour is assumed for the masonry with directions coinciding with the horizontal and vertical directions, the elastic properties can be derived along any direction (θ direction in Figure 1) [29]

$$E_{m\theta} = \left\{ \frac{\cos^4(\theta)}{E_{m0}} + \left[\frac{1}{G_{m0\text{-}90}} - \frac{2\nu_{m0\text{-}90}}{E_{m0}} \right] \cos^2(\theta)\sin^2(\theta) + \frac{\sin^4(\theta)}{E_{m90}} \right\}^{-1} \tag{4}$$

The diagonal masonry compressive strength can now be found by assuming a linear proportion between Young's modulus and compressive strengths' ratio [30]. Considering the stress-strain relationship of unreinforced masonry in Figure 3b, the maximum IP displacement, x_{max}, can be calculated [31]

$$E_{t,m\theta} = 2E_{sec,m\theta} \rightarrow E_{sec,m\theta} = f_{m\theta} / \varepsilon_{m\theta,max} \rightarrow x_{max} = \varepsilon_{m\theta,max} d_w / \cos(\theta) \tag{5}$$

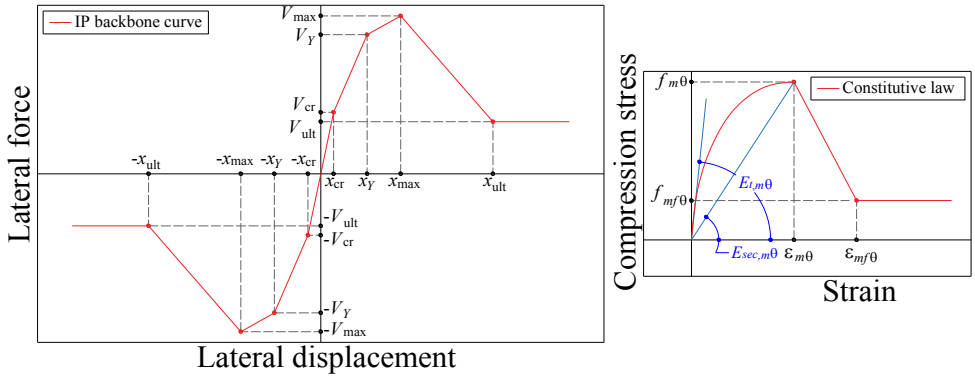

Figure 3: Constitutive relations adopted for IP behaviour of infill masonry walls.

It should be noted that this latter procedure of calculation of the masonry material elastic properties is only used when it is considered that enough real parameters are provided to adequately characterize such properties along the compression-only strut direction.

The infill wall's initial lateral stiffness, k_{0w}, can be estimated by considering double the ratio between the V_{max} and x_{max}. The IP displacement at the cracking point is computed with the values of V_{crack} and k_{0w}. The yield IP displacement, x_Y, is computed as an intermediate point between the cracking and maximum displacement [10]. The yield IP force, V_Y, is determined by assuming that the initial stiffness is modified by a factor of a (assumed 0.05),

$$V_Y = \left(V_{max} - ak_{0w}x_{max}\right) / \left(1 - a\right) \tag{6}$$

The ultimate lateral IP force, V_{ult}, and ultimate IP displacement, x_{ult}, are assumed based on the observation of the experimental results. However, values of the force are assumed to range between 20% to 50% of the V_{max}, and displacements are considered to vary between 3 and 10 times the x_{max}.

The modifications to the above-mentioned modelling strategies are briefly expounded in the next two subsections.

2.1 Modification of Furtado et al. model

Besides the different approach to the IP behaviour previously explained, a further modification to this modelling strategy is considered, being focused on the attribution of a non-linear OOP bending moment–curvature law (instead of an elastic one) to the infill wall elements'

sections at the middle of the infill panel as illustrated in Figure 4a. This backbone curve shown in Figure 4b is defined by four points (uniaxial material *pinching4* [32] in OpenSees): cracking, maximum, softening, and residual points similar to the one adopted by [11].

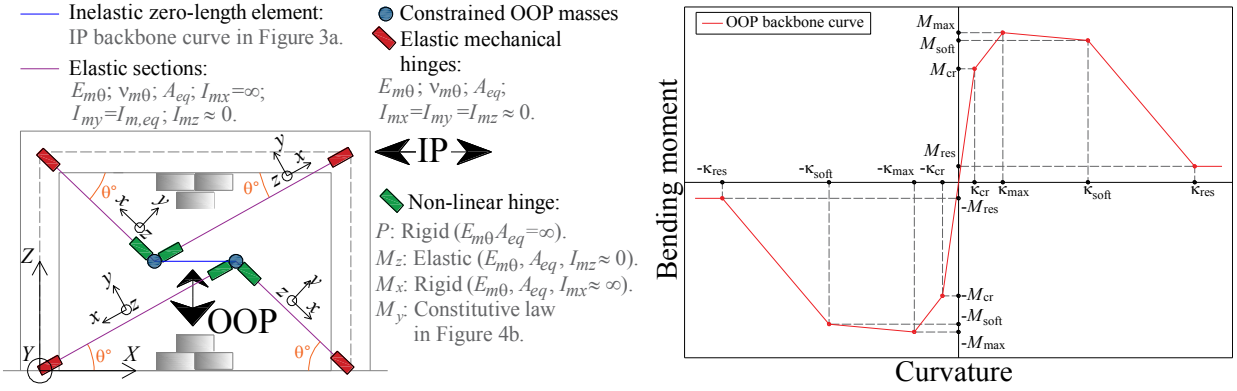

(a) Schematic representation of the model; (b) OOP moment-curvature backbone curve.

Figure 4: Modified Furtado et al. model.

The maximum point, corresponding to the maximum bending moment, is computed by adopting a similar procedure presented in [9]. This procedure follows the idea of an equivalent beam-column element spanning diagonally (derived from an original base system, i.e., a simply-supported element spanning vertically), which possesses an equivalent moment of inertia, $I_{m,eq}$,

$$I_{m,eq} = 1.644\left(\frac{d_w}{h_w}\right)^3 I \tag{7}$$

implying the first-mode effective mass (the OOP masses in Figure 4a) of 81% of the total mass of the infill. Parameter I is the moment of inertia of the original infill panel cross-section, assuming half of this value to account for cracked infill. Hence, from the equivalence between the original and equivalent systems, the maximum bending moment can be calculated by the following expression

$$M_{\max,eq} = 1.570\left(\frac{d_w}{h_w}\right) M_{\max} \tag{8}$$

in which $M_{\max}$ is the maximum moment at mid-span of a simply-supported beam (original system) with a transverse uniform distributed applied load, that can be determined as follows

$$M_{\max} = \frac{q_{OOP} d_w h_w^2}{8} \tag{9}$$

The OOP strength or capacity of the infill wall, q_{OOP}, is computed as follows

$$q_{OOP} = \begin{cases} 0.85 f_{m90}\left(\dfrac{t_w}{h_w}\right)^2 & \text{if } SL \text{ and } 2E, \\ 0.85 f_{m90}\left(\dfrac{t_w}{h_w}\right)^2 + 0.85 f_{m0}\left(\dfrac{t_w}{l_w}\right)^2 & \text{if } (WL \text{ or } ML) \text{ and } 4E. \end{cases} \tag{10}$$

The terms *WL*, *ML* and *SL* are referred to as weak layout, moderate layout and strong layout infill wall leaves, respectively, and 2*E* and 4*E* mean the infill supported on two edges and four (all) edges, respectively. These terms and corresponding equations in Equation 10 were herein chosen based on the definitions provided by Di Domenico [15]. The first expression in the system of equations (top equation) is based on the one provided by Eurocode 6 [28] (although the author in [15], modified it according to McDowell et al.'s model [33] to include the term 0.85), being more appropriate to strong infills (*SL*) that may develop one-arching mechanism being thus supported on two edges.

Di Domenico [15] considered the Eurocode 6 [28] formulation to estimate the OOP strength of infills supported on four edges (4*E*) by summing the contributions of the two arching mechanisms expected to occur in *WL* and *ML* infills. Then by performing non-linear regression analysis, the established regression coefficient values on this formulation were determined for different deformed shapes, load shapes and boundary conditions, revealing good results in predicting the OOP strength of such infills. In this study, the second expression (bottom expression) simply assumes the sum of the two arching mechanisms' contributions, by considering the same value for the stress block ($0.85f_m$ of stress distribution at the ends of the arching mechanism parts [33]) for both contributions and adjusting the definition of slenderness ratio (inverse in Equation 10) depending on the arch direction. The choice of one or another expression is herein simplified to the value of the slenderness ratio of the infill, i.e., if the slenderness value is less than 15 the first expression is used, otherwise the second expression holds.

The cracking OOP moment on the OOP backbone curve is calculated by assuming $0.70q_{OOP}$ in the calculation of the respective bending moment. The softening moment is considered as a 5% reduction of the $M_{max,eq}$ and the residual moment is taken as 15% of the $M_{max,eq}$ for simulation convergence purposes (a smaller value can be considered).

The cracking and maximum curvatures are computed using the respective moments and bending stiffnesses. The softening and residual curvatures are assumed three and fifteen times the maximum curvature, respectively (although these values can be adjusted depending on the experimental result and numerical application).

The calculation of these parameters (excluding the maximum point parameters) was carried out based on a limited study with few experimental results. Further research should establish proper relations that can characterize the OOP behaviour of a wider range of infill masonry walls.

2.2 Modification of Kadysiewski and Mosalam model

This modelling strategy considers at the centre of the infill panel, sections with fibres along the orthogonal direction to the infill wall plane. The area and position of each fibre govern the IP and OOP behaviours of the infill wall. These parameters' values are obtained by satisfying the forces interaction limit curve shown in Figure 5 and certain geometric conditions of the corresponding sections derived from the actual infill wall geometric characteristics. Further details can be found in [9].

The main modification to this modelling strategy is in the constitutive relation assumed for the fibres. The original model considers a bilinear or elastoplastic behaviour assigned to each fibre of the infill wall. In the current study, a pentalinear constitutive relation is assumed for each fibre by using the uniaxial material *pinching4* [32] in OpenSees. In contrast with the original modelling formulation, expressions to calculate the IP and OOP capacity, respectively, represented by Equations 1 and 10 are used instead in the current modified model.

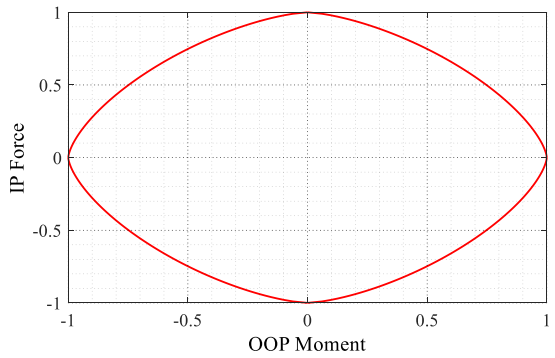

Figure 5: Interaction curve in terms of forces.

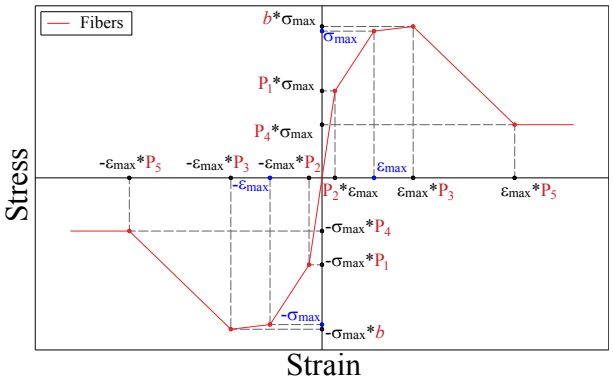

Figure 6: Pentalinear backbone curve and identification of scalar parameters.

From the sixteen parameters defining the pentalinear backbone curve (four stresses and four strains, positive and negative), twelve will be multiplied by a scalar to adjust both the IP and OOP behaviour of the infill wall. In reality, only six scalars will be needed since the response will be considered symmetric. This adjustment allows for the consideration of the initial elastic stiffness and post-yield softening behaviour verified in the infill masonry walls response while satisfying the interaction curve in Figure 5. Figure 6 shows the backbone curve and the identification of the scalar parameters for the stress-strain fibre response adjustment. It is seen that every parameter is derived from the maximum stress, σ_{max}, and strain, ε_{max}, calculated for each fibre using the procedure in [9]. The strain values are always calculated concerning the stress and the masonry Young's modulus ($\varepsilon_{max} = E_m \, \sigma_{max}$).

Parameter b will account for the strength hardening response, which in this case is assumed a very small value (nearly zero) to respect the referred interaction curve. Parameters P_1 to P_5 account for the stress-strain adjustments shown in Figure 6. However, parameters P_1 and P_2 are always set to 0.55 and 0.50, respectively.

As an example, Figure 7 shows an application of this model by using the elastoplastic material behaviour for the fibres as in the original Kadysiewski and Mosalam model. As can be verified, the use of such an approach may not be appropriate for replicating the cyclic response of frame structures with infill walls. However, in this example, the collapse-removal algorithm was not used, which could have added a steep softening branch to the response.

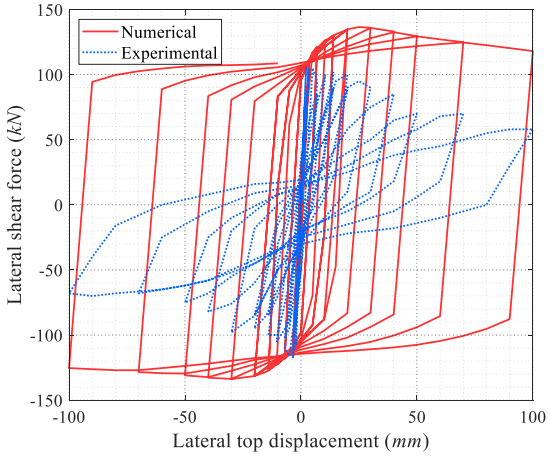

Figure 7: Kadysiewski and Mosalam model using an elastoplastic material for each fibre to replicate the cyclic response of specimen M2 in Pires and Carvalho's [13] experimental campaign.

The modified approach also allows for the further calibration of the intervenient parameters in the fibres' material constitutive relation, which can thus account for stiffness and strength degradation, and pinching effects.

Values for the remaining scalar parameters (P_3 to P_5) will be calculated (among the targets for optimization/calibration) in the next section for the different experimental results considered.

3 MODELS VALIDATION AND RESULTS

As evident in the previous brief description of the modified models, whether the original or modified Furtado et al. model [10] does not account directly for IP and OOP interaction of forces, i.e., it does not enforce this condition in the same way as the original Kadysiewski and Mosalam model [9], where the force response point would travel along the force interaction curve in Figure 5 when intersected. Instead, it includes based on the original Kadysiewski and Mosalam model, an interaction curve in terms of drifts that when reached signifies collapse, activating the element removal algorithm, which removes the collapsed infill wall elements from the model for further time-steps of the analysis.

This element removal algorithm is also included in the present modified versions of the models, although it is not activated in the process of optimization to be carried out for analysis purposes.

An optimization procedure is used similar to the one used in [16] and presented in Figure 8. This procedure makes use of a simplex algorithm where boundaries are applied [34]. Then, subsequently, a genetic algorithm (built-in function in MATLAB [21]) is implemented, which uses as an initial guess the previous solution obtained with the simplex algorithm.

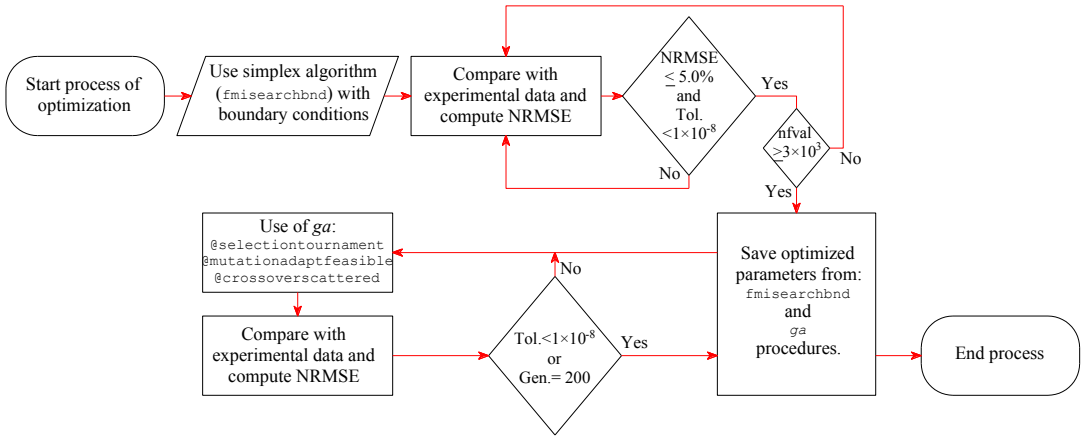

Figure 8: Flowchart of the optimization procedure used in this study.

Certain parameters are allowed to vary depending on the response to be replicated. In this sense, different experimental results are considered in this study for model validation: Pires and Carvalho [13] which considers the quasi-static cyclic analysis of RC portal frame structures with and without infill masonry walls exclusively loaded in the IP direction (Specimens used: M2 and M6); Di Domenico [15], that tested numerous portal frame specimens loaded in the IP and OOP direction in a quasi-statically manner (Specimens used: 120_OOP_4E, 120_IP+OOP_L, 120_IP+OOP_M, 120_IP+OOP_H, 120_OOP_4E_cyclic); and Negro et al. [14] which performed pseudo-dynamic tests on a full-scale RC building without infill walls and with infill walls in different configurations (Specimens used: Full-infilled wall RC building).

From here on the modified model of Furtado et al. will be named “modified model 1” and the modified model of Kadysiewski and Mosalam as “modified model 2”. The results of the optimization procedure are presented in Figures 9 to 15. For the modified model 1, 9 parameters are considered for optimization, whose results are presented in Table 1. Modified model 2 has 10 parameters for optimization. Its results are presented in Table 2. These parameters are related to the definition of the uniaxial material *pinching4* [32] in OpenSees [19, 20].

Figures 9a and 10a show the optimized response for specimens M2 and M6. These parameters shown in Table 1, correspond directly to the *pinching4* parameters defining the backbone curve in Figure 3a (always assuming from now on that the limit degradation parameters are equal to unity – *gKLim*, *gDLim*), except for the last two parameters (*dP*, *fP*), that scale the values of the last point in the backbone curve (displacement and force, respectively).

Figures 11a and 12a represent the results of the optimization of the backbone curve parameters in Figure 4b, i.e., related to the OOP behaviour of the infill using the modified model 1.

Figures 9b, 10b, 11b, 12b, 13, 14, and 15 are related to the optimization procedure using the modified model 2, thus considering the *pinching4* material parameters associated with the backbone curve in Figure 6. Table 2 shows the outcomes of the optimization, in which the last three parameters are scalars defined in the previous section (P_3, P_4, and P_5). Having the advantage of possessing only one constitutive law shared by both IP and OOP behaviours.

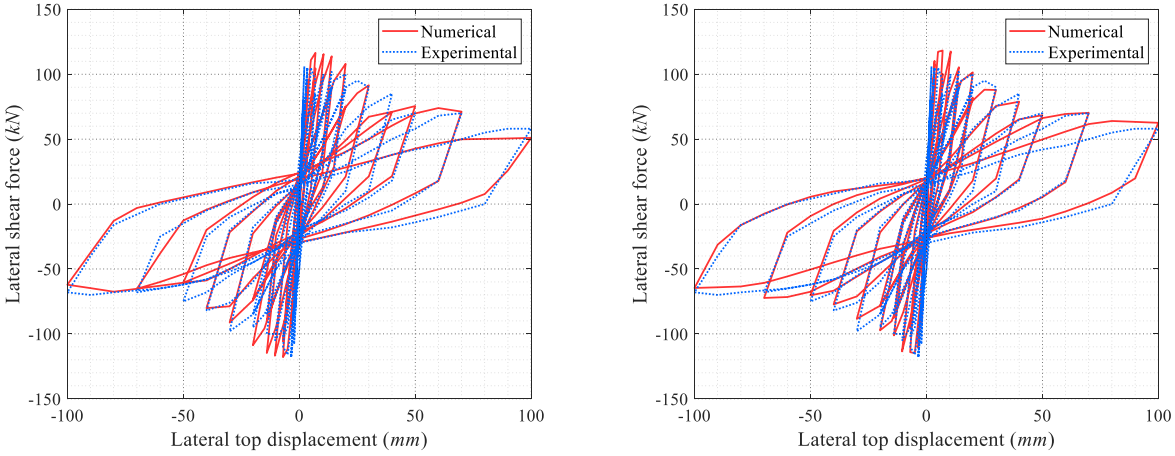

(a) Modified model 1; (b) Modified model 2.

Figure 9: Results of optimization related to specimen M2.

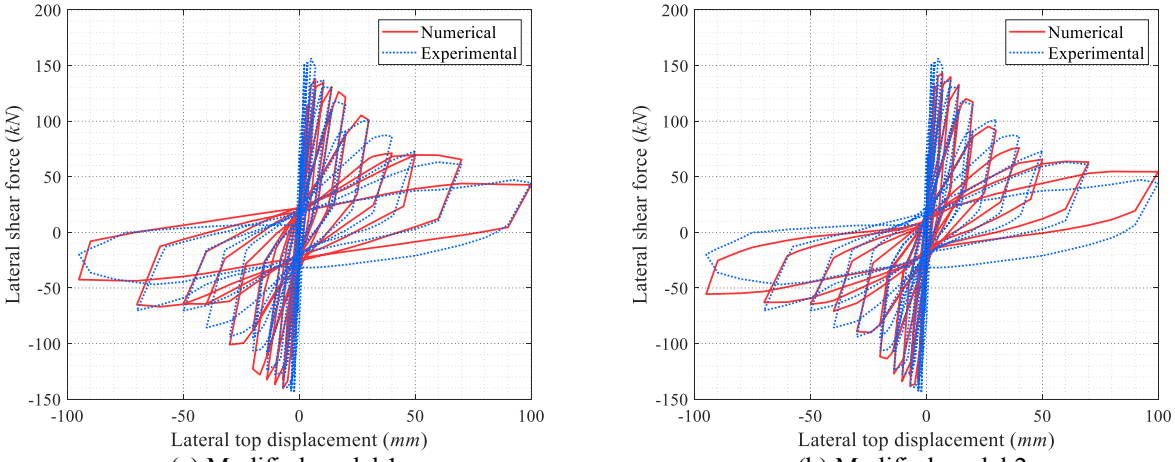

(a) Modified model 1; (b) Modified model 2.

Figure 10: Results of optimization related to specimen M6.

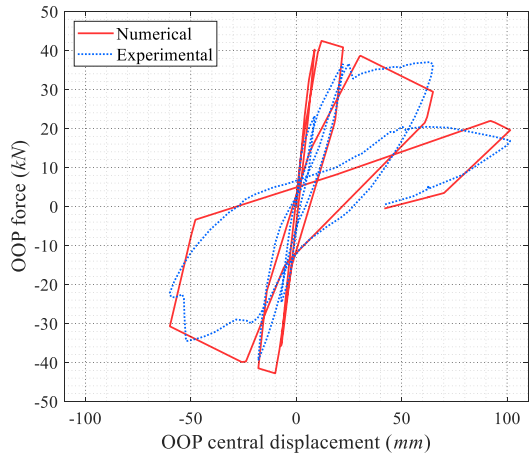

(a) Modified model 1;

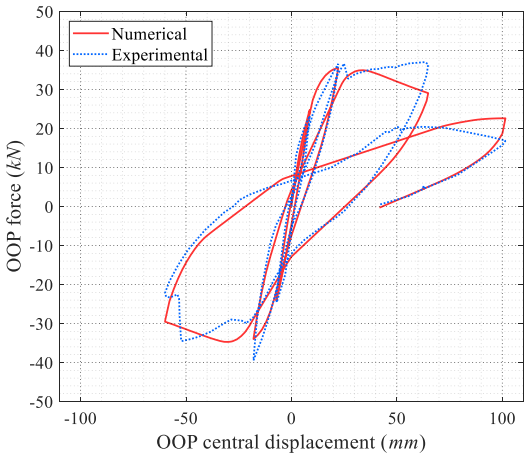

(b) Modified model 2.

Figure 11: Results of optimization related to specimen 120_OOP_4E_cyclic.

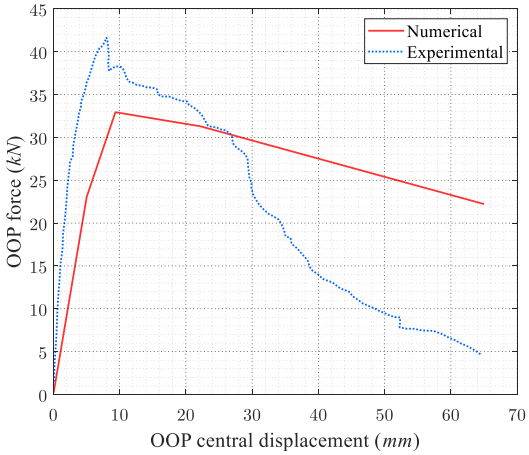

(a) Modified model 1;

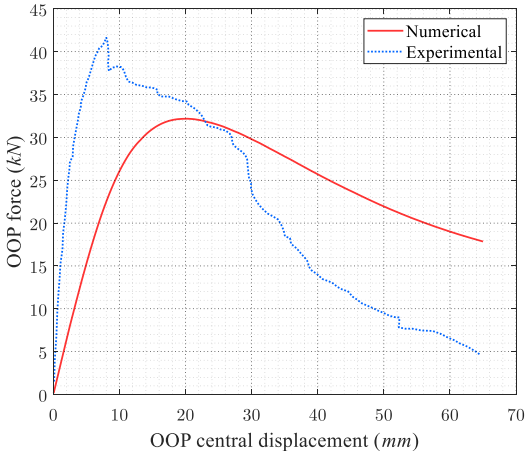

(b) Modified model 2.

Figure 12: Results of optimization related to specimen 120_OOP_4E.

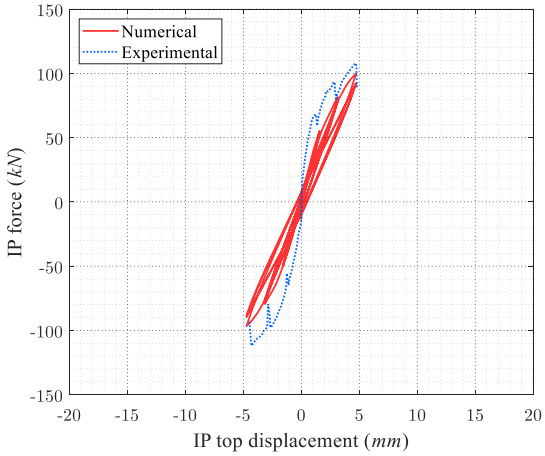

(a) Previous IP cyclic loading;

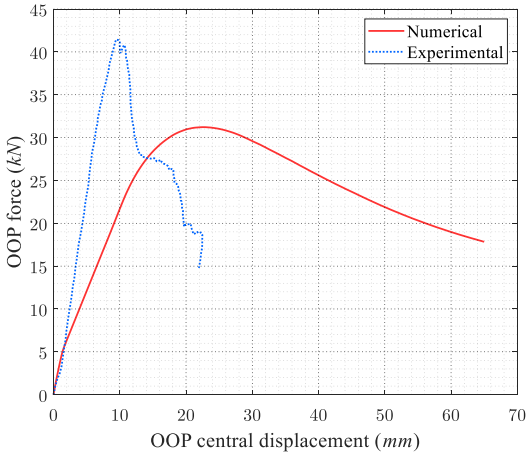

(b) Post OOP monotonic behaviour.

Figure 13: Results regarding OOP response with previous low IP damage of specimen 120_IP+OOP_L.

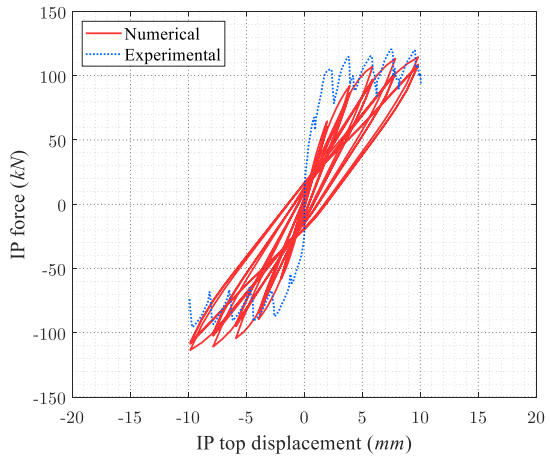

(a) Previous IP cyclic loading;

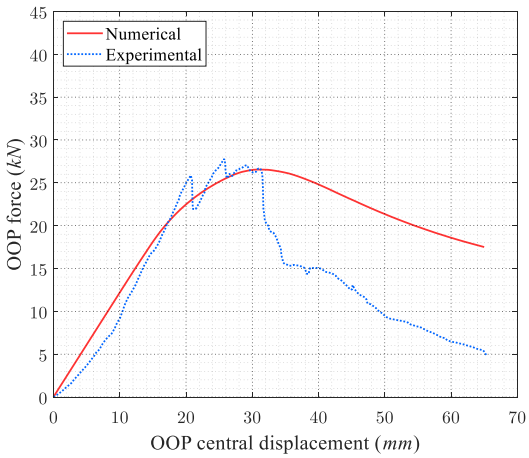

(b) Post OOP monotonic behaviour.

Figure 14: Results regarding OOP response with previous intermediate IP damage of specimen 120_IP+OOP_M.

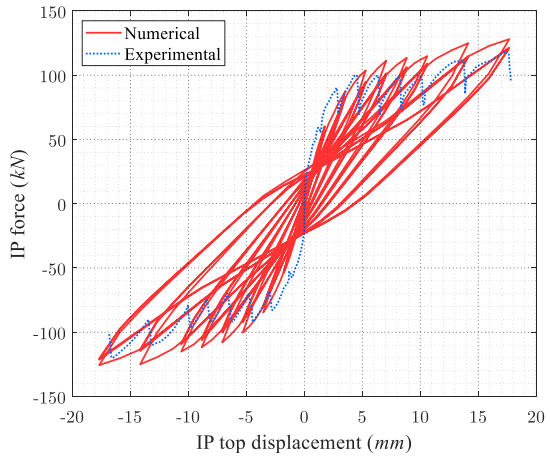

(a) Previous IP cyclic loading;

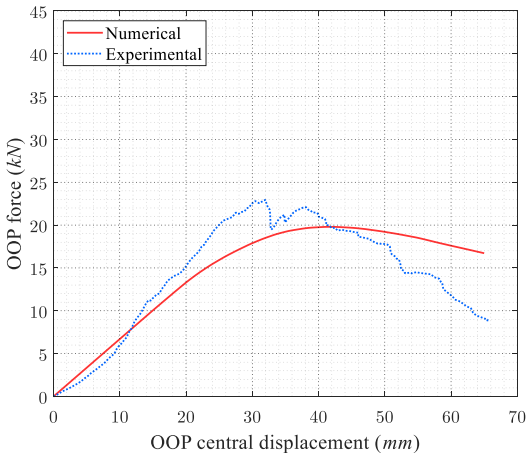

(b) Post OOP monotonic behaviour.

Figure 15: Results regarding OOP response with previous high IP damage of specimen 120_IP+OOP_H.

Figures 16 and 17 show an application of the modified models to full-scale buildings with infill walls that are only subjected to IP loads. Model parameters were manually calibrated.

In general, by graphical observation, tabled results in Table 3, and verification of the Correlation Coefficient [18] and Normalized Root Mean Square Error (NRMSE) in Figure 18, both modified models performed very well in replicating cyclic and monotonic behaviour of infill masonry walls in RC frame structures.

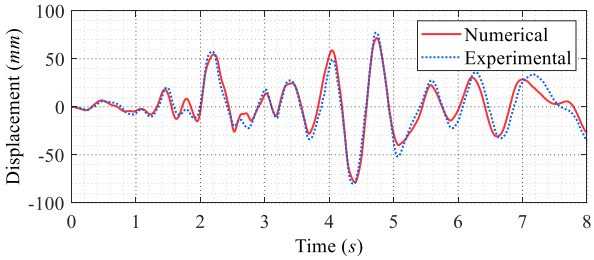

(a) Top story displacement;

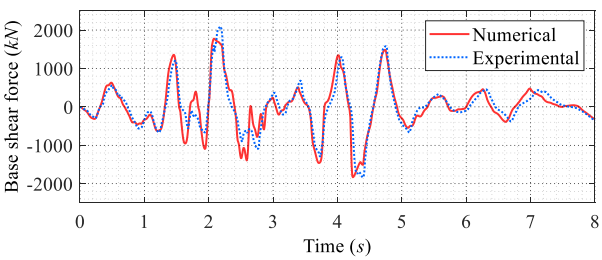

(b) Base shear force.

Figure 16: Response of the full-scale full-infilled wall building structure using the modified model 1.

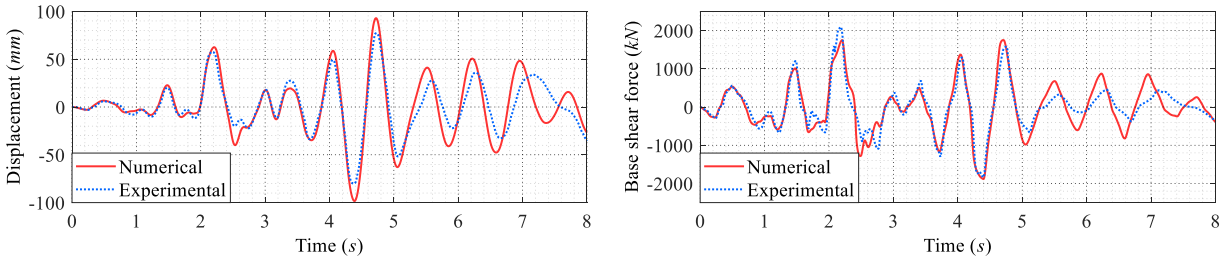

(a) Top story displacement; (b) Base shear force.

Figure 17: Response of the full-scale full-infilled wall building structure using the modified model 2.

Specimen	*rDisp*	*rForce*	*uForce*	*gK1*	*gK3*	*gD1*	*gD3*	*dP*	*FP*
M2	0.44	0.54	-0.12	0.71	0.37	0.82	1.10	5.30	0.50
M6	0.43	0.53	-0.10	0.70	0.03	0.98	1.59	5.83	0.42
120OOP4E	0.20	0.37	-0.54	1.94	0.06	0.47	0.05	22.50	0.15

Table 1: Results of the calibrated parameters for the modified model 1.

Specimen	*rDisp*	*rForce*	*uForce*	*gK1*	*gK3*	*gD1*	*gD3*	P_3	P_4	P_5
M2	0.25	0.39	-0.01	0.88	0.07	1.95	1.24	25.20	0.48	35.00
M6	0.35	0.45	-0.23	0.60	0.24	1.13	1.94	24.80	0.37	42.00
120OOP4E	-0.06	0.42	-0.33	0.05	0.05	2.00	1.46	3.10	0.25	7.60

Table 2: Results of the calibrated parameters for the modified model 2.

Model	*M2*	*M6*	*120OOP4E_Cyclic*
Modified 1	4.47 %	4.67 %	6.92 %
Modified 2	3.81 %	4.94 %	3.69 %

Table 3: Normalized Root Mean Square Errors of the different calibrations performed.

Modified model 1 is straightforward and it can represent well the IP and OOP behaviour. However, it does not enforce directly any interaction of forces between these behaviours, and hence it cannot properly consider prior damage in one direction influencing the other. Furthermore, it needs five elements in its definition, while modified model 2 only needs one. The modified model 2 can account for this interaction directly by the sequential yielding of each fibre. Figures 12 to 15 demonstrate this phenomenon very well, where previous IP loading affects the OOP behaviour by reducing it since some fibres have already yielded.

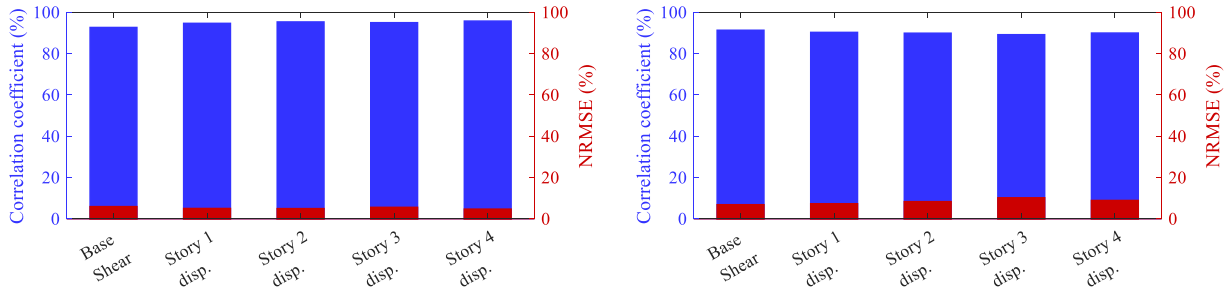

(a) Modified model 1; (b) Modified model 2.

Figure 18: Correlation between the numerical and experimental results of story displacements and base shear force time history responses.

Nevertheless, calibration of the modified model 2 may be difficult, as two-in-one behaviour is considered, which may lead to a solution fitting one behaviour and disfavoring the other. The possibility of increasing the number of fibres at the expense of computational effort can be a possible solution, even when converging problems arise. In addition, it was verified that due to the sequential yielding of fibres in this model by adopting the constitutive relation in Figure 6, may cause the infill wall to begin the softening phase without ever reaching the maximum response, i.e., without touching the interaction curve.

4 CONCLUSIONS

Two different modelling strategies were developed based on existing models, to replicate the in-plane and out-of-plane behaviour of infill masonry walls in reinforced concrete structures when subjected to horizontal loading. Generally, all responses were well predicted with either model. Nonetheless, the modified model based on Kadysiewski and Mosalam allowed for the interaction between in-plane and out-of-plane behaviour. This made it possible to satisfactorily predict the out-of-plane behaviour with prior in-plane damage, due to the sequential yielding feature of the fibres constituting the sections of the equivalent strut defining the infill panel. However, calibration can be difficult and an ideal solution may not be found due to the two-on-one behaviour defined by only one constitutive relation.

In conclusion, results showed that these modifications allowed a better reproduction of the in-plane and out-of-plane behaviour of infill masonry walls when compared with different experimental tests, being appropriate for the use in numerical models of reinforced concrete building structures, provided that the models' parameters are adequately chosen and calibrated.

Further studies should include more experimental results to aid the search for model parameters' values that better characterize the response of RC frame structures with infill masonry walls. The drawbacks of each modified model must be addressed to improve performance, stability and less computational effort for application in large structural systems subjected to different kinds of dynamic actions.

ACKNOWLEDGEMENTS

This paper is within the scope of the first author's Ph.D. degree in progress. The present research was financially supported by the Portuguese Foundation for Science and Technology (FCT) through the PhD grant reference SFRH/BD/139570/2018 under the programme POCH (N2020 – P2020) and subsidized by the European Social Fund (FSE) and national funds from MCTES. This work was also financially supported by Base Funding UIDB/04708/2020 of the *CONSTRUCT* R&D Institute on Structures and Constructions (Instituto de I&D em Estruturas e Construções), through national funds of FCT/MCTES (PIDDAC).

REFERENCES

[1] F. Nicola, C. Leandro, C. Guido, S. Enrico, Masonry infilled frame structures: state-of-the-art review of numerical modelling. *Earthquakes and Structures*, **8**(1), 225-251, 2015.

[2] P. B. Lourenço, *Computational strategies for masonry structures*. Ph.D. Thesis. Delft University, Delft, The Netherlands, 1996.

[3] M. Priestley, G. Calvi, Towards a Capacity-Design Assessment Procedure for Reinforced Concrete Frames. *Earthquake Spectra*, **7**(3), 414-436, 1991.

[4] T. Paulay, M. Priestley, *Seismic Design of Reinforced Concrete and Masonry Buildings*. John Wiley & Sons Inc., New York, USA, 1992.

[5] B. Stafford Smith, Methods for Predicting the Lateral Stiffness and Strength of Multistorey Infilled Frames. *Building Science*, **2**(3), 247-257, 1967.

[6] G. Al-Chaar, *Evaluating strength and stiffness of unreinforced masonry infill structures*. ERDC/CERL-TR-02-1, Engineer Research, and Development Center, Construction Engineering Research Lab, Champaign, IL, USA, 2002.

[7] F. Crisafulli, A. Carr, R. Park, Analytical modelling of infilled frame structures - a general review. *Bulletin of the New Zealand Society for Earthquake Engineering*, **33**(1), 30-47, 2000.

[8] G. Amato, L. Cavaleri, M. Fossetti, M. Papia, Infilled frames: influence of vertical loads on the equivalent diagonal strut model. In: *The 14th World Conference on Earthquake Engineering*, Beijing, China, October 12-17, 2008.

[9] S. Kadysiewski, K. Mosalam, *Modeling of Unreinforced Masonry Infill Walls Considering In-Plane and Out-of-Plane Interaction*. PEER Report 2008/102, Pacific Earthquake Engineering Research Center, College of Engineering, University of California, Berkeley, Berkeley, CA, USA, 2009.

[10] A. Furtado, H. Rodrigues, A. Arêde, and H. Varum, "Simplified macro-model for infill masonry walls considering the out-of-plane behaviour," Earthquake Engineering and Structural Dynamics, vol. 45, no. 4, pp. 507-524, 2016.

[11] M. Di Domenico, P. Ricci, G. Verderame, Effect of in-plane/out-of-plane interaction in infill walls on the floor spectra of reinforced concrete buildings. In: *COMPDYN2021 8th ECCOMAS Thematic Conference on Computational Methods in Structural Dynamics and Earthquake Engineering*, pp. 84-101, M. Papadrakakis, M. Fragiadakis (eds.) Streamed from Athens, Greece, 28-30 June, 2021.

[12] A. Furtado, N. Vila-Pouca, H. Varum, A. Arêde, Study of the Seismic Response on the Infill Masonry Walls of a 15-Storey Reinforced Concrete Structure in Nepal. *Buildings*, **39**(9), 2019.

[13] F. Pires, E.C. Carvalho, Cyclic Behaviour of Reinforced Concrete Frames Infilled with Brick Masonry Walls. In: *The 10th International Brick and Block Masonry Conference*, Calgary, Canada, 5-7 July, 1994.

[14] P. Negro, A. Anthoine, D. Combescure, G. Magonette, J. Molina, P. Pegon, G. Verzeletti, Tests on the Four-Storey Full-Scale Reinforced Concrete Frame with Masonry Infills: Preliminary Report. *Special Publication No.I.95.54*. European Commission. ELSA Laboratory, 1995.

[15] M. Di Domenico, Out-of-plane seismic response and modelling of unreinforced masonry infill walls. PhD Thesis. Università degli Studi di Napoli Federico II, 2018.

[16] P. Folhento, R. Barros, M. Braz-César, Optimization of the cyclic in-plane response of reinforced concrete frames with infill masonry walls using a genetic algorithm. *Controlo2022, 15th APCA ICACSC*, Caparica, Lisbon-Region, Portugal, 2022.

[17] F. Longo, G. Granello, G. Tecchio, F. da Porto, C. Modena, A Masonry infill wall model with in-plane–out-of-plane interaction applied to pushover analysis of RC frames. In: *Proceedings of 16th Brick and Block Masonry Conference (IBMAC 2016)*, Padova, Italy, June 26-30, 2016.

[18] M. H. Al Hanoun, L. Abrahamczyk, J. Schwarz, Macromodeling of in- and out-of-plane behaviour of unreinforced masonry infill walls. *Bulletin of Earthquake Engineering*, **17**, 519-535, 2019.

[19] F. Mckenna, M. Scott, G. Fenves, L. Gregory, Nonlinear Finite Element Analysis Software Architecture Using Object Composition. *Journal of Computing in Civil Engineering*, **24**(1), 95-107, 2010.

[20] M. Zhu, F. McKenna, M. H. Scott, OpenSeesPy: Python library for the OpenSees finite element framework. *SoftwareX*, **7**, 6-11, 2018.

[21] MATLAB 9.6.0.1072779 R2019a, Natick, Massachusetts, USA: MathWorks Inc., 2019.

[22] A. Neuenhofer, F. Filippou, Evaluation of Nonlinear Frame Finite-Element Models. *Journal of Structural Engineering*, **123**(7), 958-966, 1997.

[23] M. H. Scott, G. L. Fenves, Plastic Hinge Integration Methods for Force-Based Beam–Column Elements. *Journal of Structural Engineering*, **132**(2), 244-252, 2006.

[24] F. C. Filippou and G. L. Fenves, Methods of analysis for earthquake-resistant structures. In: *Earthquake Engineering: From Engineering Seismology to Performance-Based Engineering. Boca Raton: Y. Bozorgnia, and V. V. Bertero, eds.*, CRC Press, 2004, 316-393

[25] B. Scott, R. Park, M. Priestley, Stress–strain behaviour of concrete confined by overlapping hoops at low and high strain rates. *ACI Journal*, **79**(2), 13–27, 1982.

[26] Y.-H. Chen, *Seismic Evaluation of RC Buildings Infilled with Brick Walls*. PhD thesis. National Cheng-Kung University, Tainan, Taiwan, (in Chinese), 2003.

[27] FEMA 306, ATC: Evaluation of earthquake damaged concrete and masonry wall buildings, basic procedures manual, prepared by the applied technology council (ATC-33 project) for the partnership for response and recovery, published by the federal emergency management agency, Washington, D.C., USA: Report no. FEMA306, 1998.

[28] European Committee for Standardization (ECS): Eurocode 6 (EC6), EN 1996-1-1: Design of masonry structures - Part 1-1: General rules for reinforced and unreinforced masonry structures. Brussels, Belgium, 2005.

[29] R. Jones, Mechanics of composite materials. 2nd edn. Taylor & Francis, London (1998).

[30] W. El-Dakhakhni, A. Hamid, M. Elgaaly, Strength and Stiffness Prediction of Masonry Infill Panels. In: *13th World conference on earthquake engineering*. Vancouver, B.C., Canada, Paper No. 3089, 1–6 August, 2004.

[31] A. Reinhorn, H. Roh, M. Sivaselvan, S. Kunnath, R. Valles, A. Madan, C. Li, R. Lobo, Y. Park, *IDARC2D V7.0: A Program for the Inelastic Damage Analysis of Structures*. Technical Report MCEER-09-0006, State University of New York, Buffalo, USA, 2009.

[32] L. N. Lowes, M. Mitra, A. Altoontash, A Beam-Column Joint Model for Simulating the Earthquake Response of Reinforced Concrete Frames. PEER Report 2003/10, Pacific

Earthquake Engineering Research Center. College of Engineering, University of California, Berkeley USA, February, 2004.

[33] E. L. McDowell, K. E. McKee, E. Sevin, Arching action theory of masonry walls. *Journal of the Structural Division*, **82**(2), 1-8, 1956.

[34] J. D'Errico, fminsearchbnd, fminsearchcon. Available from: https://www.mathworks.com/matlabcentral/fileexchange/8277-fminsearchbnd-fminsearchcon), MATLAB Central File Exchange. Retrieved August 3, 2021.